J. Fluid Mech. (2008), *vol.* 616, *pp.* 99–109.
doi:10.1017/S0022112008004199 Printed in the United Kingdom

Morning breakup of cold pools in complex terrain

M. PRINCEVAC[1]† AND H. J. S. FERNANDO[2]

[1]Department of Mechanical Engineering, University of California, Riverside, CA 92521, USA

[2]Center for Environmental Fluid Dynamics, Department of Mechanical and Aerospace Engineering, Arizona State University, Tempe, AZ 85287–9809, USA

(Received 15 May 2008 and in revised form 17 September 2008)

Under fair weather conditions, local flow patterns in areas of complex topography are driven by diurnal heating and cooling. If the topography is basin-shaped, downslope flows occurring at night accumulate (pool) in the basin valley to form a stable layer of cold air. During the morning transition, this cold pool is destroyed by the onset of turbulent convection and upslope flow. A series of laboratory experiments was conducted to identify mechanisms responsible for the breakup of cold pools. An idealized V-shaped tank filled with thermally stratified water and heated with an approximately uniform bottom heat flux was used. Temperature measurements and dye visualization were used for flow diagnostics. Mechanisms of cold pool destruction were identified and placed in the context of previously proposed mechanisms. A new mechanism was identified, wherein a dominant intrusion emanating from the upslope flow plays a dynamically important role in cold pool destruction. The results are expected to help develop subgrid parameterizations for meso-scale weather forecasting models, which are notorious for giving poor predictions during the morning transition period in complex terrain.

1. Introduction

During the night, dense colder air carried by downslope (katabatic) winds accumulates in valleys to form a pool of stably stratified air (known as a ground-based inversion), as schematized in figure 1(*a*). Upon sunrise the surface warming causes such cold pools to dissolve, leading to a convective boundary layer near the ground, and this process is known as the morning transition. The total heat Q required to destroy an initial inversion of depth h_0 and produce an isothermal layer is given by Whiteman (1982)

$$Q = c_p \int_0^{h_0} \rho(z)[\theta_E - \theta(z)]A(z)\,\mathrm{d}z, \tag{1.1}$$

where ρ is the air density, c_p the specific heat of air at constant pressure, $\theta(z)$ the potential temperature within the inversion, θ_E the potential temperature at the top of the pool and $A(z)$ the horizontal basin area at a height z above the ground. If the amount of heat added to the valley during the diurnal cycle is smaller than Q, the inversion can persist despite daytime heating, which is typical in the wintertime of high-latitude regions (Whiteman 2000). Conversely, when the heat addition is greater than Q the cold pool is destroyed. The mechanisms of cold pool destruction are

† Email address for correspondence: marko@engr.ucr.edu

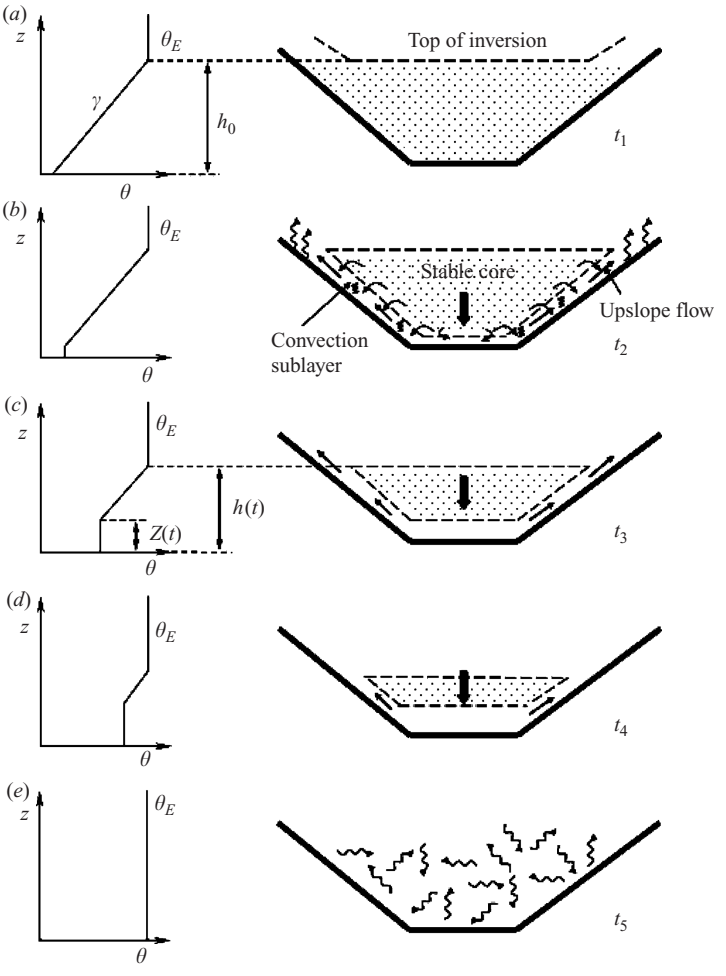

FIGURE 1. (*a*) The cold pool of air trapped in a complex topography (basin) with an initial inversion height h_0 and inversion strength γ (temperature gradient); (*b*) the development of the convective layer and upslope flow; (*c*, *d*) the development of the convective layer of depth $Z(t)$ and the descent of the stable core and the top of the inversion $h(t)$; (*e*) complete destruction of the stable core. The potential temperature profile through the middle of the basin is shown on the left (based on Whiteman 1982).

the topic of this paper, and are studied using an idealized laboratory experiment augmented by a theoretical model. Currently available mesoscale numerical weather forecasting models do not capture morning transition accurately, and thus lead to erroneous predictions of pollution transport and concentration (Lee, Fernando & Grossman-Clarke 2007). There is a critical need for better subgrid models to represent morning transition.

The existing conceptual framework proposed by Whiteman (1982) based on a composite of previous field observations is shown in figure 1. As the surface heats, a convective boundary layer of depth $Z(t)$ develops and grows via the entrainment of overlying fluid. Simultaneously, an upslope flow is initiated, transporting fluid along the boundaries and causing the top of the stable core of fluid (height $h(t)$) to descend (figures 1*b*, *c*). As the bottom of the stable layer is continuously eroded, the stable

core diminishes in size (figure 1*d*), leading to eventual destruction of the stratification (figure 1*e*).

According to Whiteman (1990, 2000), several transition scenarios are possible: (i) the initial inversion may remain stationary and the convective boundary layer can grow from below (i.e. $h(t) = h_0$ and $Z(t)$ increases); (ii) the convective boundary layer can grow to a height ($\sim$20–50 m) and remains stationary, but the upslope flow continues to cause the top of the stable core to descend while undergoing compressional heating; or (iii) a combination of (i) and (ii) is possible. Whiteman & McKee (1982) developed a thermodynamic model to predict morning transition by incorporating the above processes; the major assumption was that the stable core maintains a constant (potential) temperature gradient γ during its descent (figure 1) until the cold pool is fully broken up. Recent observations in narrow Alpine valleys (Dr. David Whiteman, personal communication), however, show that the above (i)–(iii) mechanisms are hardly present, calling for studies on alternative morning transition mechanisms.

To this end, a laboratory experiment was conducted to observe morning transition in an idealized model of a V-shaped valley. To obtain results of general validity, a spatially uniform and steady heat flux was used to mimic morning heating. The real atmosphere has topographic irregularities, synoptic and crossflows and uneven heating. Therefore, the present case represents a generic idealized flow configuration. Wide parameter ranges of heat flux, slope angle and inversion height and strength were used. The results show that in V-shaped valleys, over the parameter ranges employed, two dominant morning transition mechanisms are possible. A simple theoretical model is presented to quantify conditions for the appearance of these mechanisms and evaluated against data. Convective flow over inclines has been studied extensively (e.g. Bejan 2004) but the present work deals with breakup of background stratification by convective flow, which has not been studied in the laboratory hitherto.

2. Laboratory setup

A laboratory model of a simple two-dimensional V-shaped valley was constructed, with each incline consisting of the top surface of a closed cavity of size $100 \times 155 \times 5$ cm made of aluminum plates (figure 2*a*, *b*). The plates were held by riveted cylindrical riblets positioned between the sheets. Water of controlled temperature was circulated through the cavity, creating heat exchanger action. Each cavity had an outlet and an inlet (diameter 1.9 cm), and carefully designed flow deflectors were positioned inside the cavity to evenly distribute incoming warm water. The water entered from the top and left from the bottom of the cavity to facilitate imposing a uniform heat flux on the stratified fluid (by keeping temperature contrast between the wall and valley fluid roughly uniform). Upon start of convection, however, the temperature along the surface becomes uniform (within $\pm 0.5\,^{\circ}$C) as in the convective layer, thus providing a constant heat flux to the tank, as in Deardorff & Willis (1987). The valley walls were heated by pumping warm water through them, originating from a Branson Vapor Degreaser Type TDV-1620 reservoir with a variable thermostat. During the experiments, upon heating to the desired temperature, the water was pumped through the cavity while maintaining the temperature of the reservoir via a control system. The exit fluid from the wall cavities was recirculated through the water heater. The slope angle β could be varied by a hinge that connects two valley walls and by changing the end panels of the model valley. The valley floor

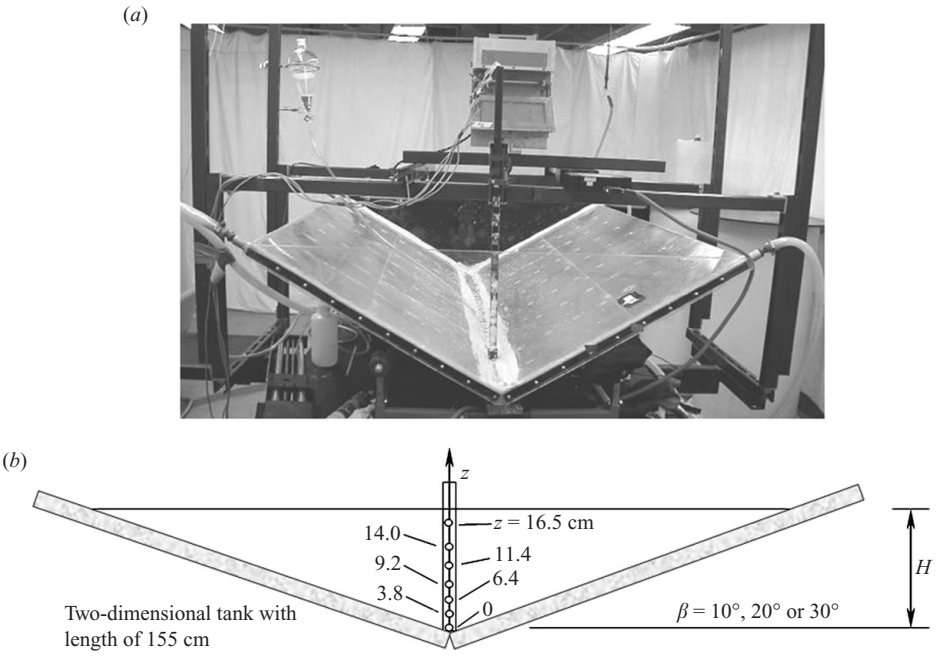

FIGURE 2. (*a*) Photo and (*b*) schematic of the V-shaped water tank used for laboratory simulation of cold pool destruction. Heights (z) of seven temperature transducers are marked.

plates were on a set of adjustable rollers. The end panels of the tank were constructed with Plexiglas (2 cm thick) for flow visualization.

The experiments were conducted with thermally stratified water as the working fluid, which has been widely used in previous slope flow and convection experiments (Deardorff & Willis 1987; Chen *et al.* 1999). First, a pool of stably stratified water of depth H ($\sim$15 to 40 cm) was prepared by filling the bottom half of the tank with water at near 0 °C and then pouring warmer water onto a floating platform. Mixing at the floater ensured that the stratification obtained is approximately linear. In some cases, gentle stirring with a rake of rods was necessary to ensure linear stratification. The vertical temperature profile in the tank was measured with a rake of seven integrated circuit temperature transducers (type AD590JF, manufactured by Analog Devices) mounted on a slender vertical rod suspended over the centre of the valley; see figure 2(*b*). The temperature sensors were rectangular with a surface contact area of $\sim 5.84 \times 2.36$ mm; the repeatability specified by the manufacturer was ± 0.1 °C with a maximum nonlinearity of ± 1.5 °C. The vertical temperature profile allowed calculation of the buoyancy frequency N (see § 4). The temperature of the incoming and outgoing water to the wall cavity was measured continuously at 0.5 Hz using the software package 'DAS-TEMP' until the complete dissolution of stable stratification; typical inlet and outlet temperatures were 60 °C and 45 °C, respectively. Initial temperature ranges of the valley fluid were from 7 °C to 17 °C in the bottom, and from 18 °C to 24 °C at the top. The temperature sensors were calibrated against a common thermometer at the initiation of each experiment. The flow visualization was performed using fluorescent dye made approximately neutrally buoyant at the valley bottom and injected there. A sharp contrast was provided for flow visualization by a black backdrop with suitable lighting, and digital snapshots were taken every 15 s.

3. Qualitative experimental observations

The experiments covered as wide a parameter range as possible, with the buoyancy flux range being $2 \times 10^{-7} < q_0 < 8 \times 10^{-6}\,\mathrm{m^2\,s^{-3}}$ and the initial stability $0.2 < N < 0.8\,\mathrm{s^{-1}}$. Based on the observations, two major inversion breakup mechanisms were identified, called CI (convection, well-defined upslope flow and some intrusions) and I (intrusion dominated). Characteristic properties of these flow regimes are:

Mechanism CI: Convective mixed layers develop near the inclined surfaces, and the mixed layers near the valley bottom merge to form a wedged convective layer that grows slowly while the upslope flow carries fluid from it along the slope (figure 3). The upslope flow reaches the density discontinuity (i.e. top of the working fluid) and flows horizontally toward the valley centre while the stable core descends and entrains into the bottom mixed layer, much like the mechanism (iii) of Whiteman (1990), finally breaking up the core. Some intrusive structures could be seen at the edges of the upslope flow, but they did not penetrate far into the stable core, nor play a role in the inversion breakup.

Mechanism I: In this case, an initial mixed layer is developed everywhere near the inclined surface as before. The flow in approximately the lower half of the slope boundary layer moved up the slope, but the upslope flow at greater heights was shut off and descended downslope. The convergence of opposing slope flows caused a strong intrusion to emanate from the slopes at near mid-depths, which propagated into the core (figure 4). As the upslope flow at lower levels of the slope was fed by the descending core, the intrusion followed a descending trajectory and entrained into the bottom mixed layer, thus increasing its thickness substantially (see arrows). The subsequent evolution was due to entrainment of (evolving) core fluid by the bottom convective layer. This is a cold-pool breakup mechanism that has not been identified before, although collapse of boundary mixed layers into stably stratified fluids in the form of intrusions is a known phenomenon (Colette, Chow & Street 2003; Lu & Turco 1994, 1995).

4. Theoretical considerations

Detailed observations made during the experiments led to the hypothesis that the formation of an intrusion near the mid-depth is due to the convergence of upslope flow maintained at smaller heights and descending alongslope flow at greater heights, as will be discussed below. As the heating starts on a long slope of angle β, a turbulent convective boundary layer develops over the slope, which also supports the upslope flow. If it is assumed to a first approximation that for small β convection is rapid and stirs the entire convective turbulent boundary layer (TBL) over its thickness δ_s and along the heated slope length L (c.f. Deardorff & Willis 1987), then the mean temperature is given by (figure 5)

$$\overline{\theta} = \frac{1}{L\delta_s}\int_0^L \int_0^{\delta_s} \theta_a(s,n)\,\mathrm{d}n\,\mathrm{d}s, \tag{4.1}$$

$$= \theta_R + \frac{\gamma}{2}\{L\sin\beta + \delta_s\cos\beta\}, \tag{4.2}$$

where γ is the initial temperature gradient and θ_a the ambient temperature given by

$$\theta_a = \theta_R + \gamma z, \quad N^2 = g\alpha\frac{\mathrm{d}\theta_a}{\mathrm{d}z} = g\alpha\gamma, \tag{4.3}$$

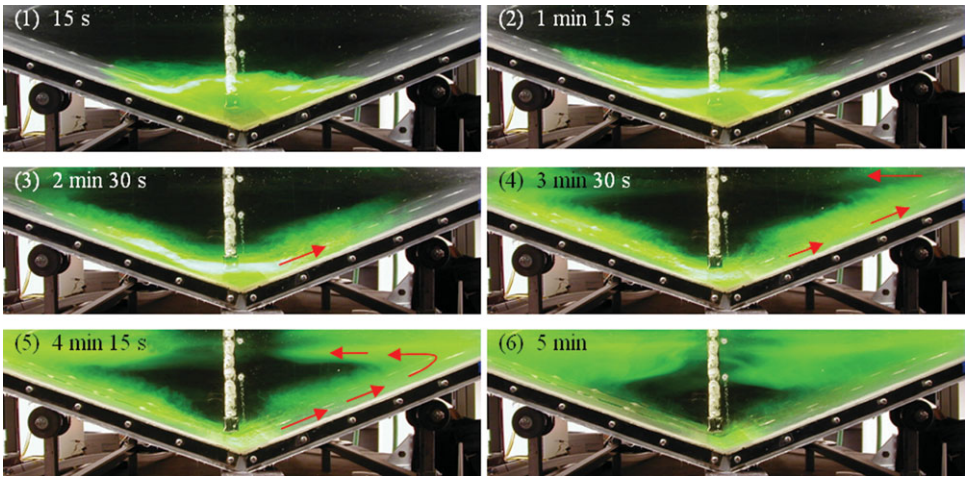

FIGURE 3. A sequence of pictures taken during an experiment with low $B = 600$ and $\beta = 20°$. Here the flow easily reaches the top of the fluid layer and initiates the recirculation and descent of the stable core. Only a few intrusions can be seen on the slopes. See arrows for flow circulation. Here $B = N^3H^2/q_0$ and β is the inclination angle of the valley slope.

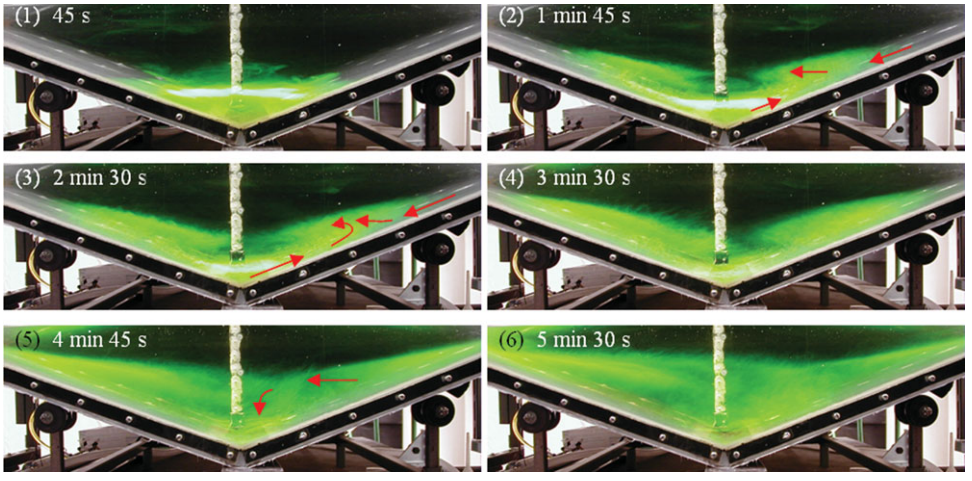

FIGURE 4. A sequence of pictures taken during an experiment with high $B = 2100$. The intrusions peeling off from approximately mid-depth of the upslope flow (detrainment) are entrained into the bottom convective layer. Here the upslope flow is weak and mainly confined to the lower heights. The intrusion is formed by the convergence of upslope flow (dyed) rising from the bottom and the sliding downslope flow (clearer fluid) from the higher levels. Owing to mixing in the convergence region, some dye diffuses to upper levels along the slope.

with α being the thermal expansivity, g the gravitational acceleration, θ_R a reference temperature and the two coordinate systems (gravity-parallel (x, z) and slope-parallel (s, n)) are shown in figure 5 with H the stratified layer depth and N the buoyancy frequency. For simplicity, two-dimensional flow is assumed. Note that the heat added during the initial transient development has been neglected, which, by calculating the buoyancy contributions from heating and turbulent mixing of a stratified layer by convection, can be shown to be valid when $B > c_1 H/\delta_s$, where $B = N^3H^2/q_0$ and $c_1 \approx 50$. This condition is typically valid in the atmosphere and in the laboratory.

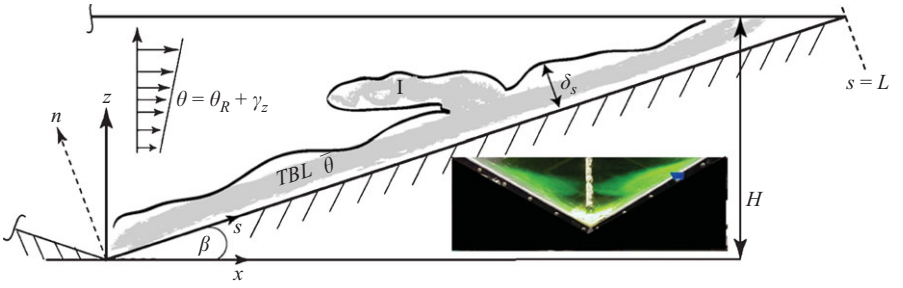

FIGURE 5. A schematic of the V-shaped valley of slope β subjected to a bottom heat flux. The initial cold pool has a uniform temperature gradient γ, and the surface heating has generated a turbulent boundary layer of thickness δ_s. Under certain conditions, a strong inversion (I) appears at approximately the mid-depth. Flow visualization is given in the inset.

The buoyancy jump between the TBL and ambient fluid at any height z, written in terms of the corresponding temperature jump $\Delta\theta$, is

$$g\alpha\Delta\theta = g\alpha(\overline{\theta} - \theta_a) \tag{4.4}$$

which becomes

$$\Delta b = g\alpha\Delta\theta = g\alpha\frac{\gamma}{2}(H - 2z + \delta_s\cos\beta), \tag{4.5}$$

$$\Delta b \approx g\alpha\frac{\gamma}{2}(H - 2z), \tag{4.6}$$

where $\delta_s/H \ll 1$ has been assumed. It is clear from (4.6) that above $z > H/2$ the buoyancy is negative, and the layer will slide down unless inertia forces of the upslope flow (U_c^2/L), where U_c is its characteristic velocity, overcome the buoyancy forces. The averaged buoyancy in this upper half is

$$\Delta\overline{b}_u = \frac{2}{H}\int_{H/2}^{H} g\frac{\alpha\gamma}{2}(H - 2z + \delta_s\cos\beta)\,\mathrm{d}z, \tag{4.7}$$

$$\Delta\overline{b}_u = -N^2H\left\{\frac{1}{4} + \frac{\delta_s}{2H}\cos\beta\right\} \approx \frac{-N^2H}{4}. \tag{4.8}$$

For this negatively buoyant layer to move up the slope, the following condition needs to be satisfied:

$$\frac{U_c^2}{L} > \frac{N^2H}{4}\sin\beta, \tag{4.9}$$

where L is the length of the slope. According to Hunt, Fernando & Princevac (2003), U_c can be written as

$$U_c = \Gamma\beta^{1/3}w_*, \tag{4.10}$$

and the TBL thickness δ_s can be parameterized as (Fernando 1987)

$$\delta_s = r(q_0/N^3)^{1/2}, \tag{4.11}$$

where Γ and r are constants and $w_* = (q_0\delta_s)^{1/3}$ is the convective (Deardorff) velocity scale. Using (4.10) and (4.11), (4.9) becomes

$$\eta\beta^{2/3} > B, \tag{4.12}$$

where $\eta = (4\Gamma^2r^{2/3})$ and $B = N^3H^2/q_0$.

If (4.12) is unattainable, the upper layers ($z > H/2$) move down the slope and the lower layers up the slope (see (4.6), $z < H/2$), thus causing a flow convergence

Slope angle (deg.)	B_{min}	B_{max}
10	107	2500
20	212	8200
30	24	5560

TABLE 1. Parameters range covered in the experiments. Neutral case, $B = 0$, was also covered for all angles.

Run No.	H (cm)	N^2 (s^{-2})	Heat flux ($kW\,m^{-2}$)	q_0 ($m^2\,s^{-3}$)	β (deg.)	B	Re
28	20	0.205	6.57	3.35×10^{-6}	20	981	10200
35	10	0.278	1.42	7.21×10^{-7}	10	2166	1220
36	10	0.157	0.52	2.66×10^{-7}	10	2497	830
40	19	0.181	5.68	2.89×10^{-6}	10	943	28500

TABLE 2. Examples of pairs with high/low values of N and q_0 but with roughly the same values of B.

on the slope at $z \approx H/2$. This leads to the emergence of a significant intrusion in the area, as observed in mechanism I. If the TBL is not well mixed, then multiple intrusions may occur, but in our experiments such intrusions were weak and only a single intrusion was dominant. As this intrusion propagates into the stratified core, it bent down somewhat because of the descent of the core fluid. In summary, the convective upslope-flow-dominated regime (CI) is expected for $\eta\beta^{2/3} > B$ and the intrusion-dominated (I) regime for $\eta\beta^{2/3} < B$, with a demarcation line between the regimes given by the critical value

$$B = B_c = C\beta^{2/3}, \tag{4.13}$$

where C is a constant to be determined experimentally. Note that C should be of order $\eta = (4\Gamma^2 r^{2/3})$, which can be estimated using previously obtained empirical constants, $\Gamma \approx 5.5$ (Chan 2001) and $r \approx 41.5$ (Fernando 1987) as $\eta \approx 1450$.

5. Quantitative experimental observations

Experiments were conducted covering as wide a range of q_0 and N as possible, and B was changed in the range $24 < B < 8200$ (see table 1). Although the Reynolds number,

$$Re = \frac{U_c \delta}{\nu} = \Gamma r^{4/3} \beta^{1/3} B^{-2/3} \left(\frac{q_0 H^4}{\nu^3} \right)^{1/3}, \tag{5.1}$$

does not explicitly appear in (4.13) because of the assumption of Reynolds number similarity, it is possible that the magnitude of Re influences the validity of parameterizations such as (4.10) and (4.11). Therefore, it was decided to conduct a number of experiments with roughly the same B but with different Re defined in (5.1); $\Gamma \approx 5.5$ and $r \approx 41.5$ were employed. Special attention was given to experiments in the proximity of transition between the regimes and to investigate whether the results are Re sensitive (see table 2). No systematic dependence on Re was identified. The Re values listed in figure 6 indicate variation over two orders of magnitude over all the experiments.

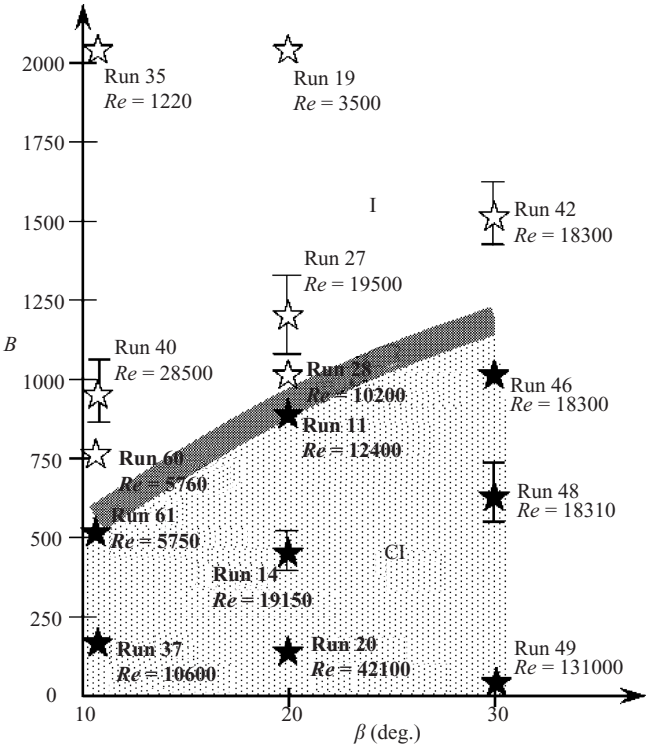

FIGURE 6. Regime diagram with the thick grey demarcation line $B_c = C\beta^{2/3}$, where the best fit gives $C = 1750$. A subset of experiments are shown with corresponding *Re*. Black stars represent experiments where convection with some intrusions (CI) was observed while white stars are experiments where the intrusions (I) were dominant. For clarity, error bars (90 % confidence) are given for several data points.

Experiments clearly indicated the existence of a critical B for the transition from CI to I, and this value increases with increasing slope angle β. Flow visualization showed that, for a given B, an increase of β increases the tendency of flow to develop weak multiple intrusions emanating from the edges of the convective boundary layer. Figure 6 is a composite of all the experimental observations together with the plausible best fit to (4.13), the empirical constant being $C = 1750$. This is indeed of the order of the estimated $\eta \approx 1450$. Plots like figure 6 can be used to predict the morning inversion breakup mechanism in narrow valleys, if q_0, N and H are available.

6. Conclusion and discussion

The morning breakup of an inversion in complex terrain was investigated using an idealized laboratory experiment. A narrow V-shaped valley with negligible bottom width and uniform surface heating was considered. Two major flow patterns were delineated CI: when the stratification is low compared to the heat flux, the flow is dominated by upslope advection (anabatic flow), accompanied by a subsidence in the middle of the valley, and the destruction of the descending stable core occurs by convective turbulence. I: when the stratification is significant compared to the heat flux, the destruction of the stable core occurs via a dominant horizontal intrusion at mid-depth and its entrainment into the bottom convective layer. The

mechanics of CI encapsulates some of the elements proposed by Whiteman (1982). In Whiteman's mechanism (i), the top of the density inversion remains stationary although entrainment progresses causing the convective mixed layer to grow, and in mechanism (ii) the convective mixed layer grows to a stationary height and remains stationary as a result of a balance between the entrainment and subsidence of the stable core. Although neither of these not observed as stand alone mechanisms, the mixed mechanism (iii) of Whiteman is similar to the CI of this paper. Mechanism I has not been identified previously, but plays an important role under certain conditions. It was found that the type of inversion breakup is determined by the parameters $B = N^3H^2/q_0$ and the slope angle β. The new mechanism involving horizontal intrusions into stable core (I) becomes important at higher values of B ($> B_c$). It is interesting to note that the formation of intrusions during evening transition on mountain slopes when q_0 is becoming weaker has been noted in the two- and three-dimensional numerical simulations of Lu & Turco (1994, 1995). When q_0 is large, the upslope flow overshoots the mountain top (chimney effect), with fully developed flow over the slope. When q_0 starts decreasing, the flow collapses (or 'stabilizes') over the slope and an intrusion is formed on the slope, roughly at the mid-depth. The present work offers a dynamical explanation for their observations in that arguably the 'stabilization' occurs above B_c. Lu & Turco, however, did not study morning transition.

The time period for morning transition as well as the heat and momentum fluxes involved in the two mechanisms are different, are their parameterizations in meso-scale numerical weather prediction models. Implementation of these mechanisms in a meso-scale model is being pursued, encouraged by the improvement of nocturnal predictions by a new parameterization dealing with stably stratified flows (Lee *et al.* 2006). Although in this preliminary study a narrow valley of negligible bottom width was used, the cold pool destruction mechanism is expected to be sensitive to the valley width/inversion height ratio, which should be a topic of future work.

This work was supported by the DOE Environmental Meteorology Program, NSF (ATM) and the Science Foundation of Arizona. We wish to thank the REU student Mr Andrew Mills, Mr Adam Christman and the referees for their help in numerous ways.

REFERENCES

Bejan, A. 2004 *Convection Heat Transfer*. John Wiley & Sons.

Chen, R. R., Berman, N. S., Boyer, D. L. & Fernando, H. J. S. 1999 Physical modeling of nocturnal drainage flow in complex terrain. *Contrib. Atmos. Phys.* **72**, 219–242.

Chan, W. C. 2001 The modeling of an anabatic flow in complex terrain. MS Thesis, Arizona State University.

Colette, A., Chow, F. K. & Street, R. L. 2003 A numerical study of inversion-layer breakup and the effects of topographic shading in idealized valleys. *J. Appl. Met.* **42**, 1255–1272.

Deardorff, J. W. & Willis, G. E. 1987 Turbulence within a baroclinic laboratory mixed layer above a sloping surface. *J. Atmos. Sci.* **44**(4), 772–778.

Fernando, H. J. S. 1987 The formation of a layered structure when a stable salinity gradient is heated from below. *J. Fluid Mech.* **182**, 525–541.

Hunt, J. C. R., Fernando, H. J. S. & Princevac, M. 2003 Unsteady Thermally Driven Flows on Gentle Slopes. *J. Atmos. Sci.* **60**(17), 2169–2182.

Lee, S. M., Fernando, H. J. S. & Grossman-Clarke, S. 2007 MM5-SMOKE-CMAQ as a modeling tool for 8-h ozone regulatory enforcement: application to the state of Arizona. *Environ. Model. Assess.* **12**(1), 63–74.

Lee, S. M., Giori, W., Princevac, M. & Fernando, H. J. S. 2006 A new turbulent parameterization for the nocturnal PBL over complex terrain. *Boundary Layer Met*. **119**(1), 109–134.

Lu, R. & Turco, R. P. 1994 Air pollutant transport in a coastal environment. Part 1: 2-D simulations of sea-breeze and mountain effects. *J. Atmos. Sci.* **51**(15), 2285–2308.

Lu, R. & Turco, R. P. 1995 Air Pollutant Transport in a Coastal Environment. Part 2: 3-Dimensional Simulations Over Los-Angeles Basin *Atmos. Environ.* **29**(13), 1499–1518.

Whiteman, C. D. 1982 Breakup of temperature inversions in deep mountain valleys: Part I. Observations. *J. Appl. Met*. **21**(3), 270–289.

Whiteman, C. D. & McKee, T. B. 1982 Breakup of temperature inversions in deep mountain valleys: Part II. Thermodynamic model. *J. Appl. Met*. **21**(3), 290–302.

Whiteman, C. D. 2000 *Mountain Meteorology: Fundamentals and Applications*. Oxford University Press.

Whiteman, C. D. 1990 Observations of thermally developed wind systems in mountainous terrain. In *Atmospheric Processes Over Complex Terrain* (ed. W. Blumen). Meterological Monographs, vol. 23 (45), pp. 5–42. American Meteorological Society